www.ioirp.com

International Journal of Innovative Research in Technology, Science & Engineering (IJIRTSE)
ISSN: 2395-5619, Volume – 1, Issue – 3. May 2015

ENHANCED RHODAMINE B DYE ADSORPTION BY GROUNDNUT SHELL ACTIVATED CARBON COATED WITH Fe_3O_4

[1]Saifullahi Shehu Imam, [2]Perumal Panneerselvam
[12]Department of Chemistry, SRM University, Kattankulathur, India.
[1]saifaz2005@yahoo.com, [2]panneerselvam1982@yahoo.com

***Abstract*— In this present study, adsorption capacity of groundnut shell activated carbon coated with Fe_3O_4 as a low cost adsorbent for removal of cationic dye, Rhodamine B (RDB) from aqueous solution was explored. The surface morphology and functional groups present were investigated by scanning electron microscope (SEM) and Fourier transform infrared (FTIR) spectroscopy. The effect of various parameters such as contact time, pH, adsorbent dosage and concentration of adsorbate were studied at ambient temperature. Equilibrium data were analysed using Langmuir, Freundlich and Temkin isotherm models. Kinetic data were studied using Pseudo-first and Pseudo-second order kinetic models and the mechanism of adsorption was described by intraparticle diffusion model.**

Keywords*— Adsorption, Groundnut shell, RDB, Kinetics, Isotherm

I. INTRODUCTION

Nowadays as a result of growing environmental awareness, the use of natural dye stuff obtained from vegetable and other animal sources have decreased substantially. They are replaced by synthetic dye stuffs produced on an industrial scale with its largest consumer being the textile industries [1]. More than 10,000 different types of dyes and pigments, with an annual production of more than 0.7 million tons are commercially available [2]. Unfortunately, during the dyeing process, a large percentage of the synthetic dye does not bind and is lost to the waste stream as residual dyes, approximately 5-10% dyes are released into the environment making the effluent highly coloured with breakdown products that are toxic, carcinogenic or mutagenic. Thus clearly, dyes are a potential hazard to living organisms [3].

Conventional waste water treatment methods for removing dyes include physicochemical, chemical and biological methods, but are very expensive and advance in technology [4]. Adsorption onto activated carbon process is one of the effective techniques that have been successfully employed for dyes removal from waste water because of its capability for adsorbing a broad range of different types of adsorbates efficiently, and its simplicity of design [4]. However, commercially available activated carbon is still considered expensive [5]. Groundnut shells are sometimes used for stock feed, but not as popular as cereal straws and legume stovers. Therefore, they can be used for the commercial production of activated carbon without much competition from livestock industry. Moreover, large quantities of groundnut shells can be obtained very cheaply from companies that are involved in shelling groundnut.

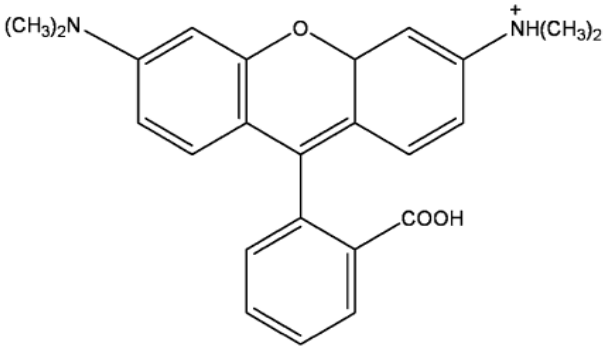

Figure 1: Chemical Structure of RDB

International Journal of Innovative Research in Technology, Science & Engineering (IJIRTSE)
ISSN: 2395-5619, Volume – 1, Issue – 3. May 2015

II. EXPERIMENTAL

A. Preparation of activated carbon

Groundnut shells were obtained from shelling units. The shells were washed with deionized water and dried in a hot air oven at temperature of 120ºC for 3 hours. The dried shells were then grounded into fine particles for easy activation. The activation procedure was carried out in a 2L beaker by thoroughly soaking the powdered material in concentrated sulphuric acid 1:2 (W/V) heated to 200ºC with continuous agitation for 1h. During this period, the water was evaporated and the mixture became slurry and started to solidify. Agitation was then stopped while heating continues until the material became a carbon like material. The resulting carbon was then allowed to cool to room temperature, washed with distilled water, soaked in dilute sodium hydroxide for 30 minutes; washed a second time with distilled water and dried in an oven. The product was crushed, sieved into sizes at 100µm and then stored in a tight bottle ready for use.

B. Preparation of Fe_3O_4-AC

The chemical precipitation technique has been used to prepare particles with homogeneous composition and narrow size distribution [5]. A complete precipitation of Fe_3O_4 was achieved under alkaline condition, while maintaining a molar ratio of Fe^{2+} to Fe^{3+}, 1:2, under inert environment. To obtain 2g of Fe_3O_4, 2.1g of $FeSO_4.7H_2O$ and 3.1g of $FeCl_3.6H_2O$ were dissolved under inert atmosphere in 80ml of double distilled water with vigorous stirring using a mechanical stirrer. While the solution was heated to 80ºC, 10ml of NH_4OH solution (25%) was added. To ensure complete growth, 10g of the prepared groundnut shell activated carbon was added and reaction continued for 30 minutes. The resulting suspension was cooled down to room temperature and then repeatedly washed with distilled water to remove unreacted chemicals. The product was dried in an oven at 50ºC for 2h, tested using a magnetic rod and then stored in a tight bottle ready for use. The reactions that occur in the production are shown in chemical equations (1) and (2).

$$FeSO_4.7H_2O + 2FeCl_3.6H_2O + 8NH_4OH \rightarrow Fe_3O_4 + 6NH_4Cl + (NH_4)_2SO_4 + 17H_2O \quad (1)$$

$$Fe_3O_4 + AC + 17H_2O \rightarrow AC\text{-}Fe_3O_4 \quad (2)$$

C. Batch Adsorption Experiments

The batch adsorption experiments were conducted to study optimum removal of colour from the dye solution. 0.2g of AC-Fe_3O_4 was added into a glass stopper conical flask containing 50ml of dye solution at 25ºC. All adsorption experiments were conducted at temperature of 303K and agitation was provided at constant rate of 100rpm. The contents were filtered using a whatman filter paper no. 42. Analysis was done using UV-Visible spectrophotometer (Elico Model No: SL210). Dye concentration in the supernatant was estimated by measuring absorbance at maximum wavelength 545nm and computing from calibration curve. The kinetic studies were carried out using a mechanical stirrer. The samples were withdrawn at predetermined time intervals and filtered. The percentage removal and amount of RDB adsorbed was calculated by the following equations.

$$Percentage\ removal\ of\ RDB = \frac{C_o - C_e}{C_o} X\ 100 \quad \text{.....(1)}$$

$$Amount\ of\ RDB\ adsorbed\ (q_e) = \frac{(C_o - C_e)\,V}{m} \quad \text{.....(2)}$$

Where C_o and C_e are the initial and equilibrium concentration of RDB (mgL^{-1}) respectively, m is the mass of the adsorbent (g) and V is the volume of RDB solution (L).

III. RESULTS AND DISCUSSION

A. Adsorbent Analysis Method

The Fe_2O_3 enriched with groundnut shell was characterized by SEM and FT-IR. The Scanning Electron Microscopy (SEM) measurements were carried out using SEM-Quanta. The images were taken with an emission current = 100 µÅ by the Tungsten filament and an accelerator voltage =10kV. Fourier transform infrared spectroscopy of the adsorbent was done by using an FT-IR spectrophotometer (Model: FT-IR Bruker IFS 66V). Spectra obtained in the range of 400 to 4000 cm^{-1} were analysed.

- *SEM Studies*

SEM is a primary tool for characterizing the surface texture, morphology and fundamental physical proportion of the adsorbent. It is useful for determining particle shape, porosity, and appropriate size distribution of the adsorbent [6-10]. SEM images for the parent activated carbon (AC), Fe_3O_4 coated activated carbon (AC- Fe_3O_4) and after RDB adsorption (AC- Fe_3O_4-RDB) are shown in figure 2. The parent activated carbon (AC) as shown in figure 2a has more active sites, while figure 2b shows the parent activated carbon completely covered with iron oxide. Figure 2c shows the SEM image, after the adsorption of RDB onto AC- Fe_3O_4. The iron oxide particles exhibit magnetic behaviour, which is depicted by more particles being adsorbed as shown in figure 2c.

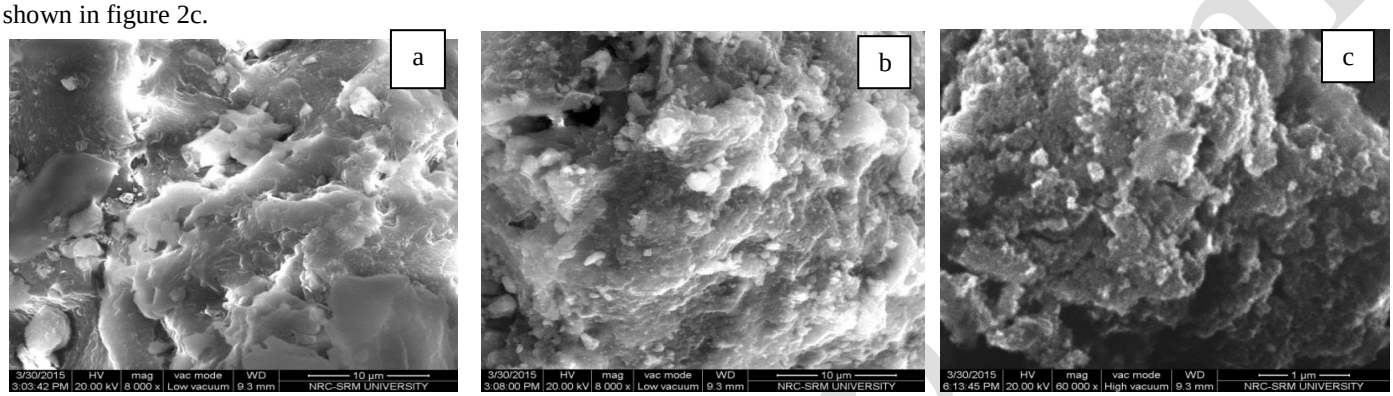

Figure 2: SEM image of (a) parent AC, (b) AC- Fe_3O_4 and (c) AC- Fe_3O_4-RDB

- *Fourier Transform Infrared Spectroscopy*

Fourier transform infrared spectroscopy of the adsorbent was done by using an FTIR spectrophotometer (Model: FTIR Bruker IFS 66V). Spectra obtained in the range of 400 to 4000 cm^{-1} were analysed. The FTIR spectra of both Parent AC and AC-Fe_3O_4 are shown in figures 3a and 3b. The spectrum of the Parent AC displayed the following bands: 3412cm^{-1}: OH and NH stretching; 2938cm^{-1}: C-H stretching in alkanes, 1631cm^{-1}: C=O stretching in amides, 1621cm^{-1}: C=C stretching in alkenes, 1208cm^{-1}: C-O stretching in ethers; 798cm^{-1} CH_2 bending in benzene derivatives [10-18]. The main oxygen groups were suggested to be carbonyl groups (such as, ketone, quinones), and phenol, ether in the parent AC. The band at 468 and 534 cm^{-1} which were associated with the in-plane and out-of-plane aromatic ring deformation vibrations common that is quite common for activated carbon. When comparing the two peaks in figures 3a and 3b, figure 3b shows that there were various functional groups detected on the surface of AC- Fe_3O_4 and a peak is observed in the Fe-O group. There are some peaks that were shifted, disappeared and new peaks were produced. Significant band decrease of functional group on the AC- Fe_3O_4 were detected at bands 1631, 1402, 1209 and 1034 cm^{-1} which corresponded to the bonded C=O stretching, stretching in quinones, stretching alkanes and C-O stretching in ethers respectively. The newer peak at 589cm^{-1} observed in figure 3b is related to the Fe-O group, and the peak around 3432 cm^{-1} in curve a was assigned to the –OH group on the surface of the magnetite. Figure 3c shows the FTIR spectrum after adsorption of RDB onto AC- Fe_3O_4. When comparing figure 3c with 3b, it can be clearly seen that most of the functional groups present on the surface get destroyed. The presence of polar functional groups on the surface is likely to confer considerable anion exchange capacity on the adsorbents [16-21].

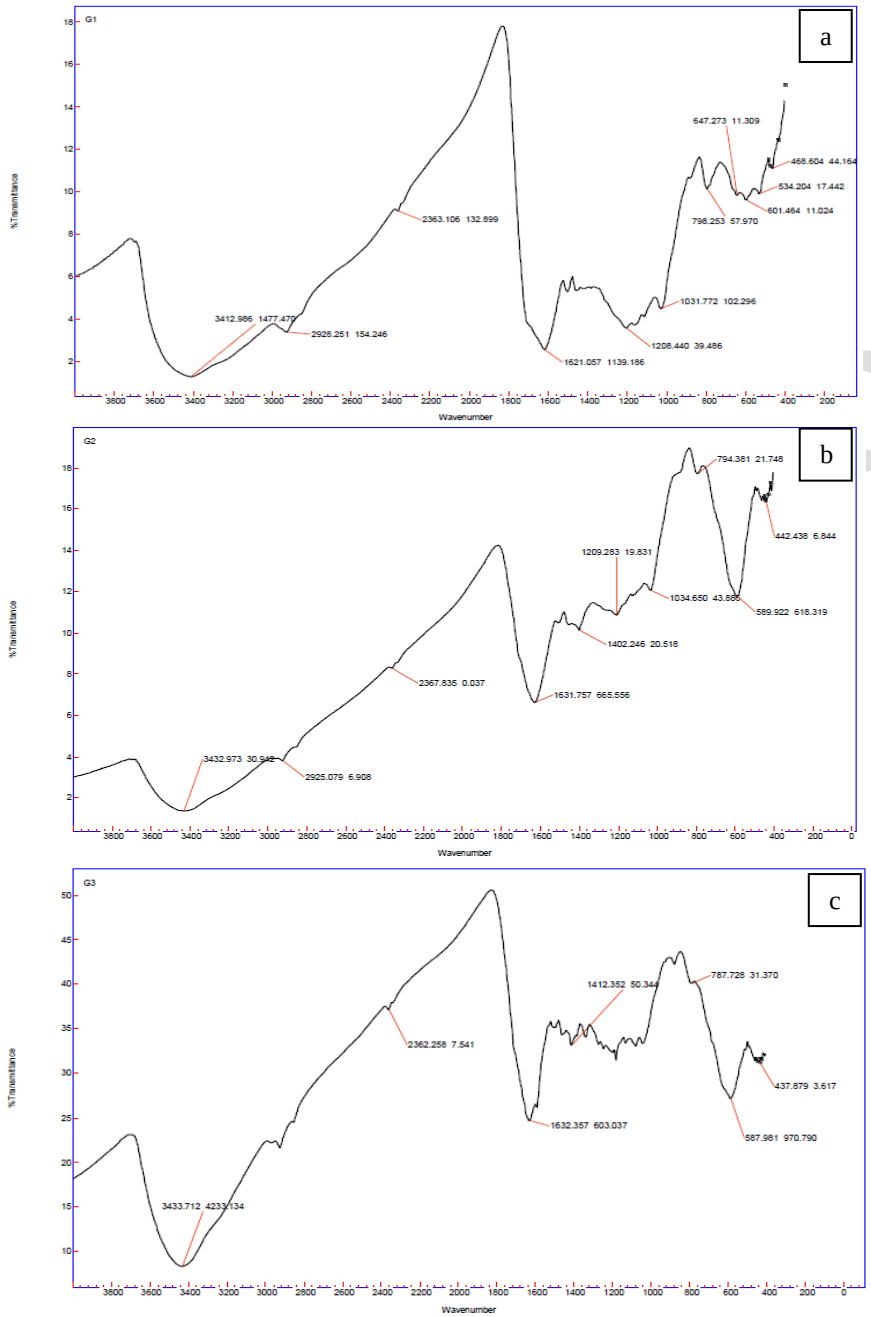

Figure 3: FTIR image of (a) parent AC, (b) AC- Fe_3O_4 and (c) AC- Fe_3O_4-RDB

B. Effect of Time

The percentage of dye adsorbed at different time interval is calculated by keeping the concentration as 100 mgL^{-1} and the mass of the adsorbent as 0.2g. From figure 4, it can be seen that the rate of adsorption was very rapid at initial period of contact time. After 120 minutes, the solution attains equilibrium [7]. The quick adsorption in the first 60 minutes is due to the high availability of adsorption sites, there after the available adsorption sites become fewer which decrease the rate of adsorption and an equilibrium state was attained. This time was taken as optimum contact time for all subsequent studies [6-7].

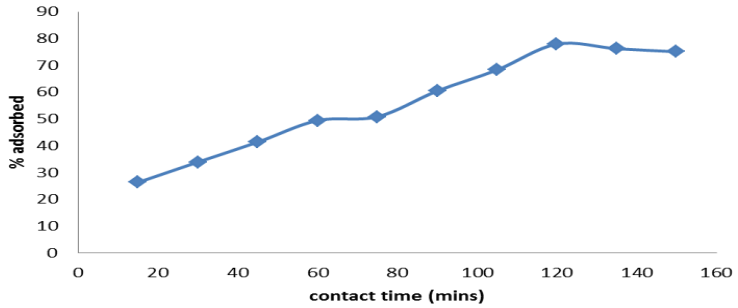

Figure 4: Effect of Contact Time

C. Effect of pH

pH of the aqueous solution is a controlling parameter in the adsorption process. The influence of pH was studied using a portable pH meter (Systronics made) by adjusting the reaction mixture to different initial pH (2 to 6) value using 0.1M Sodium Hydroxide or Hydrochloric Acid before adding the adsorbent. The pH meter was calibrated using 4.0 buffer tablet. As clearly seen in figure 5, there is high uptake at low pH values compared to the high pH values. This may be attributed to the fact that at pH value below 6, the RDB ions can enter into the pore structure, while at high pH values above 6, the zwitter ions of RDB may increase the aggregation of RDB to form a bigger molecular form (dimer) and become unable to enter the into the pore structure [8-14].

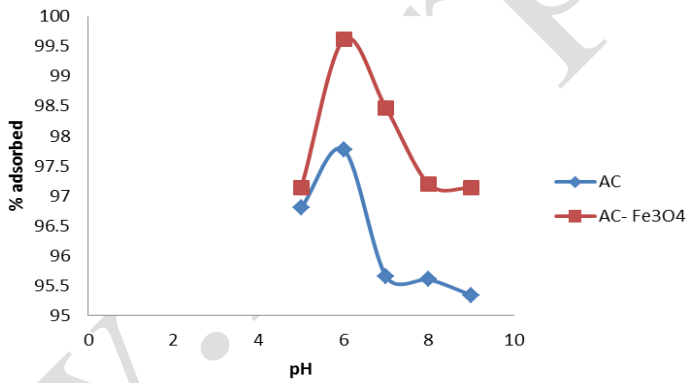

Figure 5: Effect of pH

D. Effect of AC- Fe_3O_4 Dose

This factor is used to determine the uptake capacity of an adsorbent for a given initial concentration of an adsorbate. This was studied by varying the AC- Fe_3O_4 dose (0.1 – 0.5 g/50ml) for RDB of concentration 100 mgL^{-1}. The percentage adsorption (as shown in figure 6) increases with increase in the AC- Fe_3O_4 dose. This is attributed to the increase in surface area and more adsorption sites [6]. This observation is consistent with Langmuir hypothesis of an increase competition among adsorbent particles for organic substances with increasing number of adsorbent particles per unit volume [9-10].

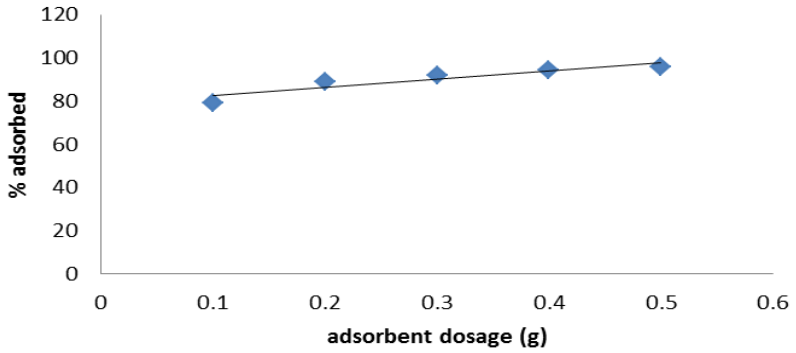

Figure 6: Effect of Adsorbent Dosage

E. Effect of Initial Dye Concentration

This was studied by varying the initial concentration of the dye, while keeping other parameters constant. It was observed (as shown in figure 7) that the percentage removal decreases with increase in dye concentration. This is due to the fact that, at low concentration, there are much available sites for adsorption whereas, with increase in initial concentration, the available sites for adsorption becomes fewer, thereby reducing the percentage removal of RDB [10-16].

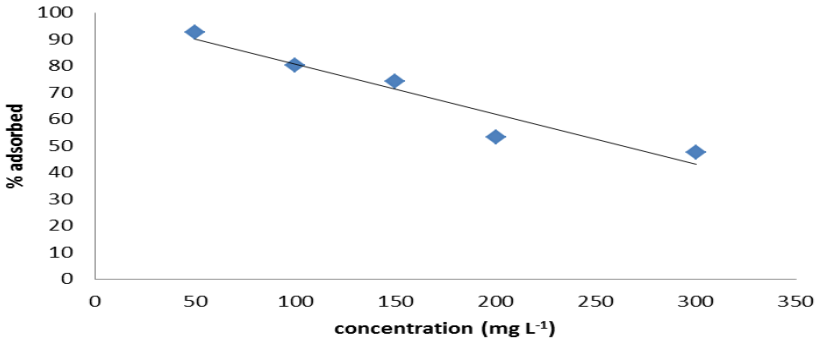

Figure 7: Effect of Initial Dye Concentration

F. Adsorption Isotherm

The adsorption isotherm indicates equilibrium relationship between the adsorbent and adsorbate [17]. The analysis of the isotherm data by fitting them to different isotherms models is an important step to find the suitable model that can be used for the designed purpose. Its applicability was judged with the regression coefficients (R^2).The isotherms used include:

- *Langmuir Isotherm*

The Langmuir isotherm was chosen for the estimation of maximum adsorption capacity corresponding to complete monolayer coverage on the adsorbent surface [18]. It applies to the cases of adsorption on completely homogeneous surfaces where interactions between adsorbed molecules are negligible. The linearized Langmuir equation was used to analyse the data. The equation is given as:

$$\frac{C_e}{q_e} = \frac{1}{K_L q_m} + \frac{C_e}{q_m} \quad \text{.....(3)}$$

Where, C_e is the equilibrium concentration of the adsorbate (mgL^{-1}), q_e is the amount of adsorbate adsorbed per unit mass of the adsorbent (mg/g), q_m and K_L is the Langmuir constants related to adsorption capacity and energy of adsorption, respectively. The more the R^2 value approaches unity, the more fitted the adsorption is to Langmuir isotherm [16].

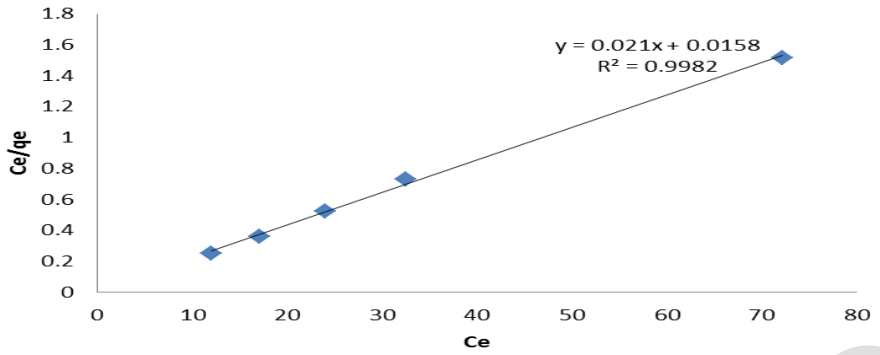

Figure 8: Langmuir Isotherm for RDB adsorption onto AC- Fe_3O_4

The essential features of the Langmuir isotherm may be expressed in terms of equilibrium parameter R_L which is a dimension less constant referred to as separation factor or equilibrium parameter.

$$R_L = \frac{1}{1+K_L C_o} \quad \text{.....(4)}$$

Where, C_o is initial dye concentration (mg/L) and K_L is Langmuir constant related to the energy of adsorption. R_L value indicates the adsorption nature to be either unfavourable if $R_L > 1$, linear if $R_L = 1$, favourable $0 < R_L < 1$ and irreversible if $R_L = 0$. The R_L was 0.204 suggesting isotherm to be favourable at concentrations studied as the value lies between 0 and 1 [16-18].

- *Freundlich Isotherm*

The Freundlich isotherm model was chosen to estimate the adsorption intensity of the adsorbent. It assumes that uptake of dyes occurs on a heterogeneous adsorbent surface that has unequal available sites with different energies of adsorption. The linear form of Freundlich equation is given as follows:

$$\ln q_e = \ln K_f + \ln C_e \frac{1}{n} \quad \text{.....(5)}$$

Where, K_f is a constant indicative of the adsorption capacity of the adsorbent (mg/g) and the constant 1/n indicates the intensity of the adsorption. Figure 9 shows linearized Freundlich isotherm for RDB adsorption onto AC-Fe_3O_4 respectively. The more the R^2 value approaches unity, the more fitted the adsorption is to Freundlich isotherm [16].

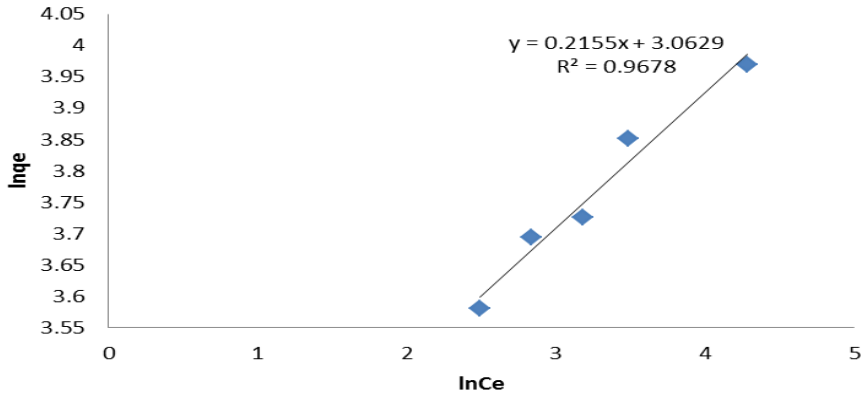

Figure 9: Freundlich Isotherm for RDB adsorption onto AC- Fe_3O_4

The magnitude of the exponent, n gives an indication of the favourability and capacity of the adsorbate/adsorbent system, where (1<n<10), represent favourable adsorption process and new adsorption sites are generated, while if n =1, then the partition

between the two phases are independent of concentration [23]. In this work, the value of n was found to be 4.64, indicating favourable adsorption.

- *Temkin Isotherm*

The Temkin isotherm model predicts a uniform distribution of binding energies over the population of surface binding adsorption [17]. The linear form of Temkin equation is given as follows:

$$q_e = B\ln A + B\ln C_e \quad \text{.....(6)}$$

where A and B are the Temkin isotherm constant (L/g) and heat of sorption (J/mol) respectively. R is the gas constant (J/mol/K), b is the Temkin isotherm constant linked to the energy parameter B as shown in equation 7:

$$B = RT/b \quad \text{.....(7)}$$

Figure 10 shows linearized Temkin isotherm for RDB adsorption onto AC-Fe_3O_4 respectively. The more the R^2 value approaches unity, the more fitted the adsorption is to Temkin isotherm [17-18].

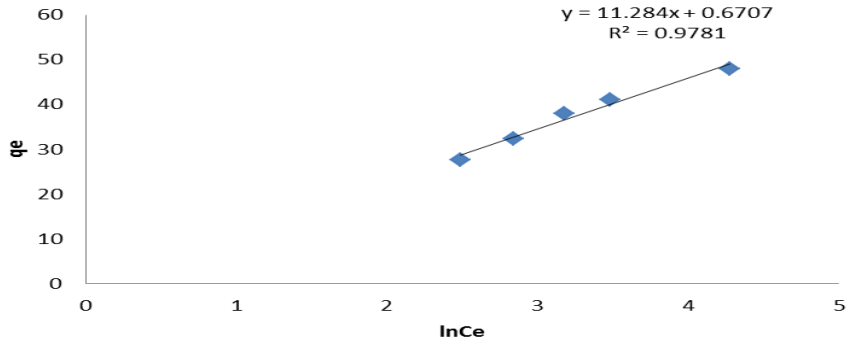

Figure 10: Temkin Isotherm for RDB adsorption onto AC- Fe_3O_4

Table 1: Isotherm Parameters for the removal of RDB onto AC-Fe_3O_4.

Langmuir isotherm			Freundlich isotherm			Temkin isotherm		
$q_m(mgg^{-1})$	$K_L(mgL^{-1})$	R^2	$K_f(mgg^{-1})$	1/n	R^2	A	B	R^2
47.61	1.3291	0.9982	21.38	0.2155	0.9678	1.06	11.28	0.9781

G. Adsorption Kinetics

The kinetics of sorption describes the solute uptake rate, which in turn governs the residence time of adsorption reaction. In order to investigate the adsorption process of RDB onto AC-Fe_3O_4, three kinetic models were used including pseudo-first order, pseudo-second order, and intra-particle diffusion models.

- *Pseudo-First Order Model*

Kinetic data were treated with the pseudo- first order kinetic model [19] .The differential equation has the following forms:

$$\frac{dq_t}{dt} = k_1(q_e - q_t) \quad \text{.....(8)}$$

Where q_e and q_t refer to the amount of the dye adsorbed (mg/g) at equilibrium and at time, t (min) respectively and k_1 is the equilibrium rate constant of pseudo- first- order adsorption (min^{-1}), Integrating equation (1) for the boundary conditions t = 0 to q_t gives:

$$\log\frac{q_e}{q_e - q_t} = \frac{k_1}{2.303}t \quad \text{.....(9)}$$

Which is integrated rate law for a pseudo- first- order equation. Equation (9) can be rearranged to obtain a linear form:

$$\log(q_e - q_t) = \log q_e - \frac{k_1}{2.303}t \quad \text{.....(10)}$$

In order to obtain rate constants, the straight line plot of log (qe-qt) against t as shown in figure 11 was used to determine the first order rate constant k_1.

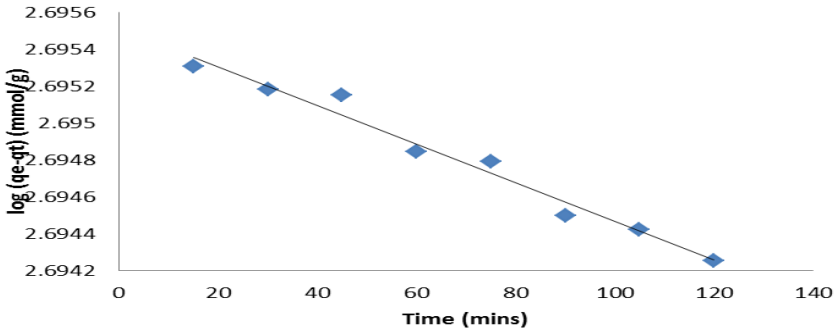

Figure 11: Pseudo-First Order Kinetics for RDB adsorption onto AC- Fe_3O_4

- *Pseudo-Second Order Model*

Kinetic data were further applied to the pseudo second order kinetic model .The differential equation has the following form:

$$\frac{dq_t}{dt} = k_2 (q_e - q_t)^2 \quad \text{.....(11)}$$

Where k_2 is the equilibrium rate constant of the pseudo- second order adsorption (g/mg min^{-1}) Integrating equation 11 for the boundary condition t = 0 to q_t, gives:

$$\frac{1}{(q_e - q_t)} = \frac{1}{q_e} + k_2 t \quad \text{.....(12)}$$

This is integrated rate law for a pseudo –second order reaction. Equation.12 can be rearranged to obtain a linear form:

$$\frac{t}{q_t} = \frac{1}{k_2 q_e^2} + \frac{t}{q_e} \quad \text{.....(13)}$$

The kinetic plots of t/q_t versus t for RDB removal is presented in figure 12. The relationship is linear, and the correlation coefficient (R^2) suggests a strong relationship between the parameters and also explains that the process of the sorption of RDB follows pseudo- second order kinetics. The product $k_2 q_e^2$ is the initial sorption rate represented as $h = k_2 q_e^2$.

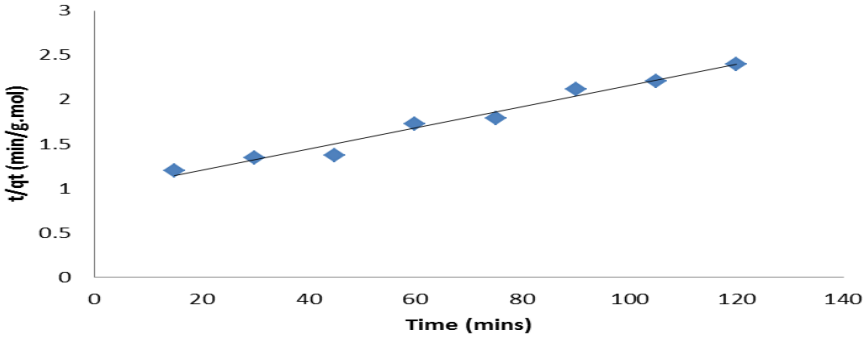

Figure 12: Pseudo-Second Order Kinetics for RDB adsorption onto AC- Fe_3O_4

- *Intra-particle Diffusion Study*

The intra-particle diffusion model was applied to identify important of pore diffusion in the adsorption process. The mathematical expression of intra-particle diffusion model is:

$$q_t = K_{int} t^{0.5} + C \quad \text{.....(14)}$$

Where, K_{int} is the intra-particle diffusion constant (mg g^{-1} $min^{-0.5}$) and the intercept (C) reflects the boundary layer effect. If the rate limiting step is intra-particle diffusion, then the graph drawn between q_t vs. $t^{0.5}$ should yield a straight line passing through the origin. The slope give the value of the intra-particle diffusion constant (K_{int}) and the value of C gives an idea about the thickness of the boundary layer. The values of K_{int} were calculated from the slope of as shown in figure 13 and presented in table 2.

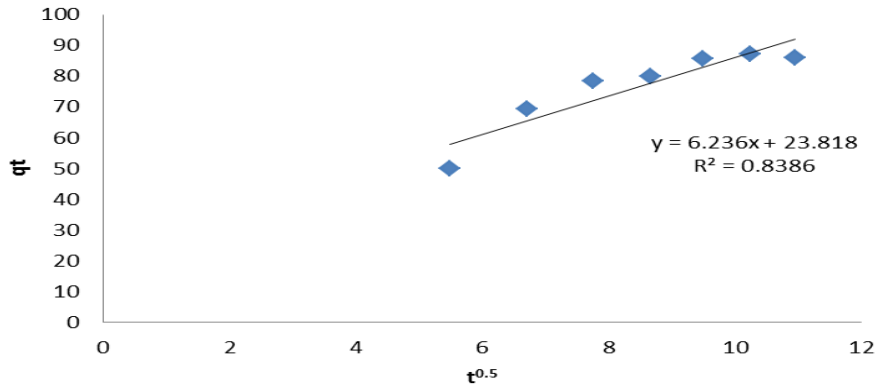

Figure 13: Intra-Particle Diffusion Plot for RDB adsorption onto AC- Fe_3O_4

Table 2: Kinetic Parameters for the removal of RDB onto AC-Fe_3O_4.

Pseudo-first order			Pseudo-second order			Intra-Particle diffusion		
$k_1(min^{-1})$ $x10^{-5}$	q_e(mg g^{-1})	R_1^2	q_e(mg g^{-1})	k_2 (g^{-1}mg min)$x10^{-4}$	R_2^2	K_{int}(mg g^{-1} $min^{-0.5}$)	C	R^2
2.303	500.61	0.9748	84.03	1.0350	0.9762	6.236	23.818	0.8386

IV. Conclusion

The use of groundnut shell activated carbon coated with Fe_2O_3 has better potential than raw groundnut shell activated carbon as a low cost adsorbent for the removal of RDB from aqueous solutions. The effect of various parameters such as contact time, pH, adsorbent dosage and dye concentration was studied. Maximum adsorption of RDB from aqueous solutions occurred at pH of 6. Adsorption increased with increasing dose of adsorbent and decreased with increasing initial RDB concentration. The experimental data shows high association with Langmuir but not Freundlich isotherm model and Temkin isotherm model. Kinetic study reveals that, the reaction order fits with pseudo second order. The process is economically feasible and easy to carry out.

Acknowledgements

The authors are grateful to Nanotechnology Research Centre, SRM University for carrying out SEM analysis.

References

[1] Weber, E.J., Adams, R.L., Chemical and sediment mediated reduction of the azo dye Disperse Blue 79. Environmental Science & Technology, 1995, 29, 1163-1170.

[2] Easton, R. R., The Dye Makers View Color, in Dye House Effluent (Ed: P.Cooper), The Alden Press, Oxford, UK 1995, p. 9.

[3] Rindle, E., Troll, W.J., Metabolic reduction of benzidine azo dyes to benzidine in the Rhesus monkey. Journal of National Cancer Institute, 1975, 55, 181.

[4] Juang R.S., Wu F.C. and Tseng R.L., Characterization and use of activated carbons prepared from bagasse for liquid-phase adsorption. Colloids and Surfaces A: Physicochemical and Engineering Aspects, 2002, 201, 191-199.

[5] Ahmad, A.A., Hameed, B.H. and Aziz, N., Adsorption of direct dye on palm ash: kinetic and equilibrium modeling. Journal of Harzardous Materials, 2006, 094, 1-10.

[6] Chakraborty, S., De, S., DasGupta, S., and Basu, J.K. Adsorption study for the removal of basic dye: experimental and modeling. Chemosphere, 58, 2005, 1079-1089.

[7] Hashem, F. S., Removal of methylene blue by magnetite-covered bentonite nano-composite, Eur. Chem. Bull., 2013, 2(8), 524-529.

[8] Laurent, S., Forge, D., Port, M., Roch, A., Robic, C., Vander Elst, L. and Muller, R.N., Magnetic iron oxide nanoparticles: synthesis, stabilization, vectorization, physicochemical characterizations and biological applications, Chem. Rev. 2008, 108, 2064-2110.

[9] Porselvi, E. and Krishnamoorthy, P., Adsorptive removal of Rhodamine-B by agricultural waste, Oriental Journal of Chemistry, 2013, 29, 719-723.

[10] Abechi, E.S., Gimba, C.E., Uzairu, A., and Kagbu, J.A., kinetics of adsorbtion of methylene blue onto activated carbon prepared from palm kernel shell, Archives of Applied Science Research, 2011, 3, 154-164.

[11] Abou-Gamra, Z.M. and Medien, H.A.A, Kinetics, Equilibrium and Thermodynamic studies of Rhodamine B adsorption by low cost biosorbent sugar cane baggase, Eurr. Chem. Bull, 2013, 2, 417-422.

[12] Yoshida, H., Fukuda, S., Okamato, A. and Kataoka, T., Water Sci. Technol., 1991, 23, 1667-1676.

[13] Nwabanne, J.T. and Igbokwe, P.K., Thermodynamic and Kinetic Behaviours of Lead (II) Adsorption on Activated Carbon derived from Palmyra palm nut, International Journal of Applied Science and Technology, 2012, 2, 244-254.

[14] Kansal, I., Walia, T. P. and Suman, J., Removal of Rhodamine B by adsorption on walnut shell charcoal. Journal of surface science and technology, 2008, 24(3-4), 179-193.

[15] Khan, T. A., Sangeetha, S. and Imran, A., Adsorption of Rhodamine B from aqueous solution onto acid activated mango (Magnifera indica) leaf powder: Equilibrium, Kinetic and Thermodynamic Studies. Journal of Toxicology and Environmental Health Sciences, 2011, 3(10), 286 – 297.

[16] Hossain, M. A., Hao, H. N., Guo, W. S. and Nguyen, T. V., Removal of Copper from Water by Adsorption onto Banana peel as Bioadsorbent. International Journal of Geomate, 2012, 2(2), 227 – 234.

[17] Rahimi, M. and Vedi, M., Langmuir, Freundlich and Temkin Adsorption Isotherms of Propranolol on Multi-Walled Carbon Nano Tube. Journal of Modern Drug Discovery and Drug Delivery Research, 2014, V1I3.DOI: 10.15297/JMDDR.V1I3.01

[18] Igwe, J. C. and Abia, A. A., Adsorption isotherm studies of Cd(II), Pb(II) and Zn(II) ions bioremediation from aqueous solution using unmodified and and EDTA-Modified Maize Cob, Ecletica Quimica, 2007, 32(1), 33 – 42.

[19] Ho Y.S., 'Citation review of Lagergren kinetic rate equation on adsorption reaction', Scientometrics., 2004, Vol.59, pp.171-177.

[20] Vinoth, M. et al., Removal of Methyl Orange from Solutions Using Yam Leaf Fibers, International Journal of Chem Tech Research, 2010, 2(4), 1892-1900.

[21] Tsai, W. T. et al., Adsorption of acid dye onto activated carbons prepared from agricultural waste bagasse by $ZnCl_2$ activation, Chemosphere 2001, 45, 51.

[22] Panneerselvam, P., Morad, N., and Tan, K.A. Magnetic nanoparticle (Fe3O4) impregnated onto tea waste for the removal of nickel(II) from aqueous solution. Journal of Hazardous Materials. 186(2011) 160-168

[23] Karthikeyan, S., Sivakumar, P., and Palanisamy, P. N. Novel activated carbons from agricultural wastes and their characteristics. E-journal of chemistry, 2008, 409-426.